RESEARCH ARTICLE

Improving genomically recoded *Escherichia coli* to produce proteins containing non-canonical amino acids

Jessica G. Perez[1,2] | Erik D. Carlson[1,2] | Oliver Weisser[1,2] | Camila Kofman[1,2] |
Kosuke Seki[1,2] | Benjamin J. Des Soye[1,2] | Ashty S. Karim[1,2] |
Michael C. Jewett[1,2,3,4]

[1] Department of Chemical and Biological Engineering, Northwestern University, Evanston, Illinois, USA

[2] Chemistry of Life Processes Institute, Northwestern University, Evanston, Illinois, USA

[3] Center for Synthetic Biology, Northwestern University, Evanston, Illinois, USA

[4] Simpson Querrey Institute, Northwestern University, Chicago, Illinois, USA

Correspondence
Michael C. Jewett, 2145 Sheridan Road, Tech E-136, Evanston, IL 60208-3120, USA.
Email: m-jewett@northwestern.edu

Abstract

A genomically recoded *Escherichia coli* strain that lacks all amber codons and release factor 1 (*C321.ΔA*) enables efficient genetic encoding of chemically diverse non-canonical amino acids (ncAAs) into proteins. While *C321.ΔA* has opened new opportunities in chemical and synthetic biology, this strain has not been optimized for protein production, limiting its utility in widespread industrial and academic applications. To address this limitation, the construction of a series of genomically recoded organisms that are optimized for cellular protein production is described. It is demonstrated that the functional deactivation of nucleases (e.g., *rne*, *endA*) and proteases (e.g., *lon*) increases production of wild-type superfolder green fluorescent protein (sfGFP) and sfGFP containing two ncAAs up to ≈5-fold. Additionally, a genomic IPTG-inducible T7 RNA polymerase (T7RNAP) cassette into these strains is introduced. Using an optimized platform, the ability to introduce two identical N_6-(propargyloxycarbonyl)-$_L$-Lysine residues site specifically into sfGFP with a 17-fold improvement in production relative to the parent strain is demonstrated. The authors envision that their library of organisms will provide the community with multiple options for increased expression of proteins with new and diverse chemistries.

KEYWORDS
amber suppression, genomically recoded organism, non-canonical amino acids, orthogonal translational system, protein production

1 | INTRODUCTION

The genetic code is a universal cipher that describes how mRNA codons are translated into proteins. Of the 64 available codons, 61 encode the twenty canonical amino acids with the remaining three (UAA, UAG, UGA) responsible for signaling termination of protein synthesis.[1] This biochemical principle extends through all kingdoms of life and for a long time was considered immutable. However, by the late 1970s, variations in the genetic code, such as the reassignment of these codons to other amino acids, had been discovered.[2] Today, over twenty variations to the standard genetic code[3] have spurred interest in utilizing these variations to encode non-canonical amino acids (ncAAs). Expanding the set of amino acids available for co-translational incorporation by the ribosome opens opportunities to site-specifically introduce new chemistries into proteins and has the potential to transform how we synthesize materials, study protein structure, and understand the translation system.[4–8] Indeed,

the site-specific incorporation of ncAAs into proteins has been utilized for biophysical studies,[9,10] creating new biocatalysts,[11] synthesizing proteins containing post-translational modifications,[12–14] and understanding translational processes and its evolution over time.[15]

Currently, over 200 ncAAs have been incorporated into proteins co-translationally.[16,17] These ncAAs include non-canonical α-amino acids (e.g., p-azidophenylalanine, fluorescent amino acids), as well as cyclic and backbone-extended (e.g., β-, γ-, δ-) monomers, among others.[18–28] Co-translational incorporation of ncAAs into proteins is most often achieved in cells by amber suppression whereby the amber stop codon (UAG) is reprogrammed and used to encode a ncAA through the activity of a ncAA-specific orthogonal translation system (OTS).[29] In general, OTSs are composed of two key components: (i) a suppressor tRNA that has been modified to decode the amber codon (o-tRNA) and (ii) an aminoacyl-tRNA synthetase that has been engineered to specifically recognize a ncAA of interest and aminoacylate it to the o-tRNA (o-aaRS).[30] These components are orthogonal in that they interact principally with a ncAA of interest and have little crosstalk with the native translation components. In practice, these orthogonal components are typically expressed from a plasmid, such as pEVOL,[31] which encodes an o-tRNA as well as two copies of the associated o-aaRS. In the presence of their cognate ncAA, these orthogonal components facilitate the repurposing of amber codons as open channels encoding the ncAA.

Historically, a key limitation to OTSs for ncAA incorporation using amber suppression has been premature truncation of the recombinant protein at the UAG amber codon due to the activity of endogenous release factor-1 (RF-1). During translation, RF-1 recognizes and binds at amber codons, subsequently activating hydrolysis of peptidyl-tRNA to release the peptide chain.[32] Thus, when attempting amber suppression, the inherent competition between RF-1 and ncAA-o-tRNAs at amber codons can cause inefficient incorporation of ncAAs and premature truncation, reducing the modified protein yield. Within the last decade, this interference was addressed with the construction of an *Escherichia coli* strain lacking all 321 UAG amber stop codons and RF-1, termed *C321.ΔA*. The amber codon is completely orthogonal in this strain and is freed for total dedication to encoding an additional ncAA.[33] Other approaches and strains have also been reported.[34,35] *C321.ΔA* has an increased ability to incorporate multiple ncAAs as compared to other *E. coli* strains, enabling many applications,[13,36–38] such as biocontainment.[38] However, compared to standard commercially available protein production strains, like BL21(DE3), *C321.ΔA* is derived from the K-strain *MG1655* and has not yet to our knowledge undergone strain development for improved protein production.

In this study, we sought to improve the utility of *C321.ΔA* by introducing genomic mutations and a robust, inducible expression system to enhance the strain's protein production utility. Given our previous successes in improving protein production in *E. coli* systems by removing negative effectors,[39–41] we targeted DNAase *endA*,[36,42] RNAases *rne*,[43] and *rnb*,[44,45] and proteases *lon*[46] and *ompT*[46] for functional inactivation in *C321.ΔA*. Protein expression of *C321.ΔA* mutant strains was tested with two different OTS systems capable of encoding a ncAA at the UAG codon: (i) an engineered *Methanocaldococcus jannaschii* tyrosyl-tRNA synthetase/suppressor tRNA pair[31] for incorporating

p-azido-L-phenylalanine (pAzF) and (ii) the wild-type *Methanosarcina mazei* pyrrolysyl-tRNA synthetase (PylRS)/suppressor tRNA pair for incorporating a pyrrolysine (Pyl) analog, N_6-(propargyloxycarbonyl)-L-Lysine (ProCarb). These two systems were chosen for their different species origin and varied use within the synthetic biology community. While various applications of the pAzF OTS have been reported,[37,41,47,48] PylRS is used less frequently likely due its difficulty being expressed recombinantly.[49,50] We show that deletion of nuclease and protease genes in the strain increases production of superfolder green fluorescent protein (sfGFP) containing two UAGs by 2.3- and 5.6-fold with pAzF and ProCarb, respectively. Next, we introduced the T7 promoter system[51,52] into *C321.ΔA*, given the advantages of high recombinant protein expression using this system. We present the construction of several strains featuring an isopropyl β-D-1-thiogalactopyranoside (IPTG) inducible T7 RNA polymerase (T7RNAP) cassette and demonstrate up to a 17-fold improvement in production of sfGFP containing 2 ProCarb residues using these strains. We envision that the library of organisms described here will be an important resource and provide the community with multiple strain options for expression of proteins containing ncAAs with increased protein yield.

2 | RESULTS AND DISCUSSION

2.1 | Functional deactivation of proteases and nucleases enhances sfGFP production in C321.ΔA

We hypothesized that reducing the activity of negative effectors of protein synthesis (e.g., proteases and nucleases) would increase protein production in *C321.ΔA*. To test this hypothesis, we prepared *C321.ΔA* derivatives featuring combinatorial functional deactivations of two proteases, two RNAses, and one DNAse using multiplex automated genome engineering (MAGE)[53] (Figure 1A; Table 1). The Lon protease was deactivated using a mutagenic MAGE oligonucleotide to remove its promoter, similar to the Lon protease mutation found in *BL21(DE3)*.[54] The point mutation D103A was introduced into *ompT* to eliminate proteolytic activity while maintaining its structural motifs in order to preserve OmpT's possible chaperone function.[55,56] RNAse E, encoded by *rne*, was truncated by inserting a stop codon at residue 131 (*rne131*), a mutation which was previously found to increase mRNA half-life.[43,57] RNAse II (encoded by *rnb* and involved with mRNA degradation[58]) and Endonuclease I (encoded by *endA* and capable of generating breaks in double-stranded DNA[59]) were similarly truncated by inserting a stop codon followed by a frameshift mutation in the first quarter of their open reading frames.[53] Starting with the parental strain *C321.ΔA*, these mutations were made in single, double, some triple, and some quadruple combinations. Mutations were screened by multiplex allele-specific colony (MASC) PCR[60] or colony PCR and confirmed by DNA sequencing. The average doubling times for the MAGE-modified strains were measured in 2x YT media and were determined to be within 12% of the parental strain (Figure 1B), suggesting that the gene disruptions did not drastically affect cellular fitness. However,
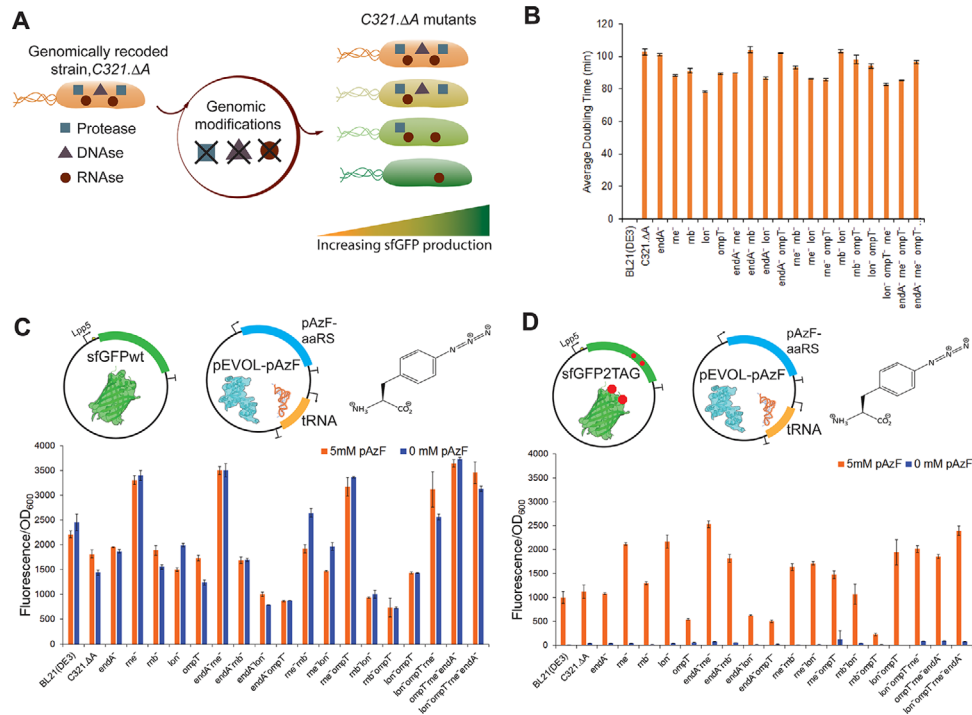
FIGURE 1 Functional inactivation of nucleases and proteases creates robust, high protein production strains for ncAA incorporation. (A) Mutagenic oligonucleotides were introduced into *C321.ΔA*, targeting two proteases (*lon* and *ompT*), two RNAases (*rne* and *rnb*), and a DNAase (*endA*) for functional inactivation. Through multiple rounds of MAGE, several *C321.ΔA* mutants were generated. (B) *C321.ΔA* mutant strains were grown at 32°C in 2x YT media in a sterile 96-well polystyrene plates. OD_{600} was measured every 10 min for 12 h. Error bars represent the standard deviation of biological duplicates and technical triplicates. (C) The protein production capability of the modified *C321.ΔA* strains were analyzed by expressing sfGFP-wt, regulated by a strong endogenous promoter pLpp5, and the pAzF OTS expressed on pEVOL-pAzF. For all conditions 1 mM IPTG, 0.02% arabinose and 5 mM pAzF (orange bars) or 0 mM pAzF (blue bars) were added at OD_{600} 0.6–0.8. (D) Modified *C321.ΔA* strains were analyzed for the ability to suppress two amber codons in sfGFP at positions 190 and 212 in the presence (orange) or absence (blue) of 5 mM pAzF. For (C) and (D) error bars represent one standard deviation for biological triplicates and technical triplicates

TABLE 1 Proteases and nucleases targeted in this study

General function	Gene	Specific function	Mutation	Phenotype	Ref.
DNA stability	*endA*	Endonuclease I	GGATGT 748 TAACTGA	Truncated at 748 nt	[42]
RNA stability	*rnb*	RNase B	GGT 584 TAACTGA	Truncated at 584 nt	[43]
	rne	RNase E	GACGCC 632 TAACTGA	Truncated at 632 nt	[61]
Protein stability	*lon*	ATP-dependent protease	Removal of promoter	Unknown	[62]
	ompT	Outer membrane protease VII	D103A	Elimination of proteolytic activity	[55,56]

growth rates, as well as protein expression levels, are likely to vary in more demanding growth conditions. For example, doubling time varies in top-performing strains when grown in M9 media (Figure S1). In M9 media, more variation in cell growth rates were observed likely because minimal media is more burdensome on metabolic processes. Additionally, Kakkar et al.[28] found higher growth rates and cell yields in synthetic media versus LB media when expressing ncAA-containing nisin, a lanthipeptide with antibacterial activity, using a *C321.ΔA* mutant.

To assess the protein production capacity of *C321.ΔA* and its mutants, we first transformed all strains with the pLpp5-sfGFP-wt plasmid, which expresses wild-type sfGFP protein (sfGFP-wt) off a

strong IPTG-inducible endogenous promoter, Lpp5[63] along with a pEVOL plasmid encoding the OTS for *p*-azidophenylalanine (pAzF)[31] (Figure 1C). The strains were grown, IPTG was added to induce sfGFP-wt expression, and sfGFP was quantified as a measure of fluorescence/O.D.$_{600}$. The *rne$^-$* mutant had the strongest impact on sfGFP-wt expression, implying that mRNA stability may be the largest limitation for expression of sfGFP-wt in *C321.ΔA*. Interestingly, the mutation combination most similar to *BL21(DE3)*, *lon$^-$ ompT$^-$*, expressed sfGFP-wt at levels 44% less than *BL21(DE3)*. This observation was not explored further, but it most likely stems from the inherent differences between B- and K-strains. Furthermore, we
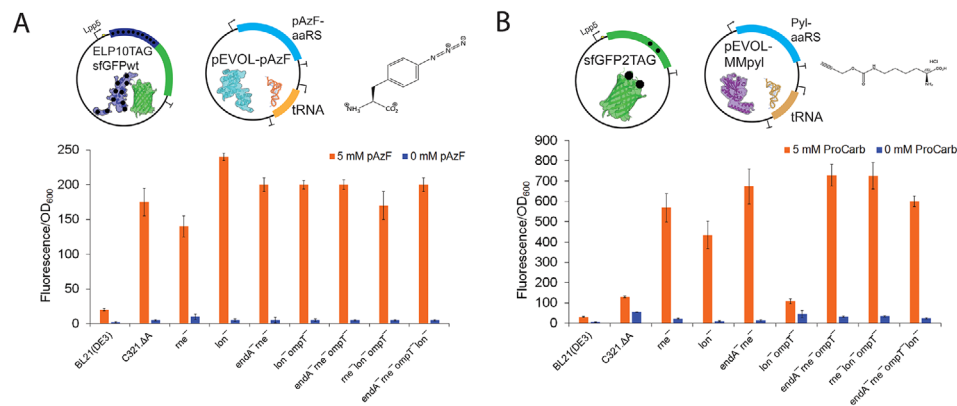
FIGURE 2 Reducing protease and nuclease activity improves multiple-site ncAA incorporation across OTSs. (A) ELP containing 10 amber codons and fused to sfGFP-wt at its C-terminus was expressed with pEVOL-pAzF in top *C321.ΔA* mutants. For all conditions 1 mM IPTG, 0.02% arabinose and 5 mM pAzF (orange bars) or 0 mM pAzF (blue bars) were added at OD_{600} 0.6–0.8. (B) Expression of sfGFP containing two amber codons for incorporation of ProCarb using the Pyl OTS was tested in top *C321.ΔA* mutants. For all panels error bars represent one standard deviation for biological triplicates and technical triplicates

observed that the addition of *endA⁻* to strains containing *rne⁻* added a minor boost in sfGFP-wt expression. Ultimately, the top mutants for expression of sfGFP-wt were *rne⁻*, *endA⁻rne⁻*, and *ompT⁻rne⁻endA⁻*, with the top mutant outproducing both *BL21(DE3)* and the parental strain by 2.6-fold.

We next explored whether the *C321.ΔA* mutant strains could better incorporate ncAAs during protein expression by using an sfGFP-expressing construct containing two amber stop codons (sfGFP-2UAG) located at position N212 and D190 in the loop regions of sfGFP to avoid negative impact to fluorescence[64] (Figure 1D). In this case, full-length sfGFP expression and fluorescence is dependent on the successful incorporation of pAzF at each amber codon. In the absence of pAzF, any fluorescence measured results from non-specific incorporation at amber codons. Under these conditions, BL21(DE3)'s ability to express sfGFP-2UAG is reduced compared to *C321.ΔA* likely a result of RF-1 being active in *BL21(DE3)*. As was the case with sfGFP-wt, the *rne⁻* strain and several mutations combined with *rne⁻* demonstrated increased productivity. The top-performing mutant was *rne⁻endA⁻* with a 2.3-fold improvement as compared to the parental strain. Comparable in performance, *lon⁻ompT⁻rne⁻endA⁻* was the next top-performing mutant. The absolute protein expression results showed a similar improvement trend as the normalized fluorescence data (Table S1).

To test the limits of these systems, top-performing mutants for both sfGFP-wt- and sfGFP-2UAG-expression were tested for the ability to incorporate pAzF at 10 amber codons. Elastin-like polypeptide (ELP) containing 10 UAGs at positions 20, 35, 50, 65, 80, 95, 110, 125, 140, and 155 was fused to sfGFP-wt at the N-terminus. In this case, all 10UAGs in the ELP must be suppressed for the sfGFP-wt moiety to be expressed and produce fluorescence. Top *C321.ΔA* mutants were co-transformed with pLpp5-ELP10UAG-sfGFP-wt and the pEVOL-pAzF plasmid (Figure 2A). The advantage of the genomically recoded strain over *BL21(DE3)*, which contains RF-1, to incorporate multiple ncAAs was especially pronounced here. None of the mutants in this case dis-

played a significant improvement compared to *C321.ΔA*; however, the system showed a 12-fold improvement over *BL21(DE3)*. This suggests the ability of OTS components to incorporate ncAAs, rather than the strain's protein production capability, is the limiting factor under these conditions.

We next tested conditions where mRNA and protein stability may be a limitation by expressing sfGFP2UAG in the presence of a pEVOL plasmid encoding the Pyl OTS system from *Methanosarcina mazei* (pEVOL-MMpyl)[65] (Figure 2B). Because there is no commercial source of Pyl and the ncAA is tedious and expensive to synthesize,[66] we used the pyrrolysine derivative ProCarb in these experiments. We observed that the *C321.ΔA* mutants had a dramatic improvement over *C321.ΔA* and BL21(DE3) for expression of sfGFP containing two ProCarbs. The top mutant, *endA⁻rne⁻ompT⁻*, showed a 5.6-fold improvement compared to the parental strain. These results demonstrate the advantage of reducing protease and nuclease activity when using o-aaRSs with known solubility issues such as PylRS.[49,50] These results also suggest that top performing *C321.ΔA* mutants will likely vary depending on the OTS being used. However, because our study only explored genomic mutations and not mutations of the OTS systems, we suspect that ncAAs with similar incorporation efficiencies to the pAzF and ProCarb would likely result in similar top performing strains (e.g., p-acetyl-l-phenylalanine (pAcF)[31] compared to pAzF incorporation).

3 | Genomic introduction of a T7 RNA polymerase cassette increases utility of *C321.ΔA*

After improving protein production capabilities in *C321.ΔA*, we wanted to further enhance the utility of this platform strain by providing transcriptional tuning capabilities. Transcriptional tuning is a powerful tool for efficient recombinant protein production in *E. coli*. Many challenges such as product toxicity, formation of inclusion bodies, and metabolic
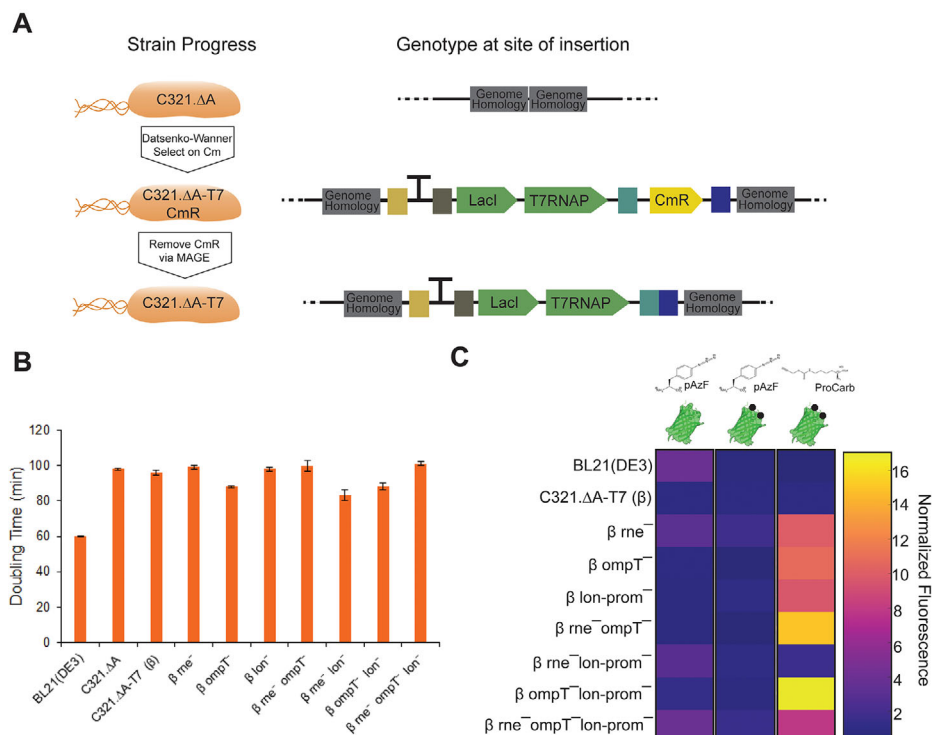
FIGURE 3 Genomic insertion of the T7RNAP cassette improves the utility of *C321.ΔA* mutant strains. (A) The T7RNAP cassette was inserted into top *C321.ΔA* mutant strains using the Datsenko-Wanner method. After recovery, transformed cells were plated on LB plates containing 34 μg/mL chloramphenicol, selecting for strains that incorporated the T7RNAP cassette. The selectable marker was then removed through several cycles of MAGE. The resultant strains were termed *C321.ΔA-T7*. (B) Strains were grown at 32⁰C in 2xYT media in a sterile 96-well polystyrene plates. OD$_{600}$ was measured every 10 min for 12 h. Error bars represent biological duplicates and technical triplicates. (C) The heat map depicts normalized fluorescence (Fluorescence/OD$_{600}$) for various reporter proteins relative to *C321.ΔA-T7(β)* within each vertical condition. Column 1: pET28a-sfGFP-wt + pEVOLpAzF + 5 mM pAzF + 1 mM IPTG + 0.02% Arabinose; Column 2: pET28a-sfGFP2UAG + pEVOLpAzF + 5 mM pAzF + 1 mM IPTG + 0.02% Arabinose; Column 3: pET28a-sfGFP2UAG + pEVOL-MMpyl + 5 mM ProCarb + 1 mM IPTG + 0.02% Arabinose. Normalized Fluorescence data is shown in Figure S3 and S4

burden are associated with non-optimal (too high or too low) levels of recombinant protein expression. Tunable expression systems allow for the adjustment of recombinant protein expression using a small molecule inducer to maximally exploit the cell's metabolic capability. Thus, the ability to tune recombinant protein expression is a staple for many protein expression projects. Within this realm, use of the T7RNAP within *BL21(DE3)* is the most popular approach for producing proteins due to the enzyme's high activity, tunability, and orthogonality. To use this system, a gene of interest is cloned behind a T7 promoter and recognized exclusively by the phage T7RNAP encoded on the genomic DE3 cassette and induced by the addition of IPTG.[46] This allows for highly productive and orthogonal recombinant protein expression that is tunable by controlled addition of IPTG. To leverage the power of the T7RNAP in *C321.ΔA*, a synthetic T7RNAP cassette was synthesized by amplifying T7RNAP from the BL21(DE3) genome and adding an upstream terminator (to transcriptionally isolate the cassette), a CmR gene as a selectable marker, and 45 bp of genomic homology to the genomic insertion site on the 5′ and 3′ end to facilitate incorporation into the genome (Figure S2). Using λ-red mediated homologous recombination,[60,67] the cassette was inserted into the top *C321.ΔA* mutant strains. Using MAGE, the CmR marker was

removed, and finally the full cassette and insertion site were verified by sequencing to yield a series of *C321.ΔA-T7* strains (Figure 3A).

To test functionality of the T7RNAP cassette, a reporter plasmid expressing sfGFP-wt or sfGFP-2UAG regulated by a T7 promoter was transformed into the *C321.ΔA-T7* strains along with pEVOL-pAzF and the ability of the strains to express sfGFP using the T7RNAP was assessed. Here, all strains including BL21(DE3) expressed the reporter proteins at levels much lower than sfGFP-wt/2UAG expression regulated by Lpp5 (Figure S5). Because T7 systems often utilize pET plasmids, the reporter plasmids were switched to a pET28a backbone.[68] With the new plasmids, BL21(DE3)'s expression of sfGFP-wt (Figure S6A) increased to near the same levels as expression of pLpp5-sfGFPwt. However, expression of sfGFP-wt, directed by T7RNAP, remained lower in the *C321.ΔA* mutants.

We hypothesized that T7RNAP-based expression in *C321.ΔA* could be improved by introducing genomic mutations similar to those present in BL21 (DE3) and its derivatives. To test this, we reconstructed the *C321.ΔA* strains containing T7RNAP by addition of the T7RNAP cassette into *C321.ΔA* (to yield strain *β*), followed by the combinatorial inactivation of *rne*, *ompT*, and *lon*. The doubling times and final OD$_{600}$ of the resulting strains in 2xYT media at 32°C were within 18% of the

parental strain (Figure 3B; Figure S7). When assessing T7RNAP-driven expression using these strains, we observed an increase in productivity of 2.2- and 3.1-fold for sfGFP-wt/pAzF and sfGFP-2UAG/pAzF, respectively (Figure S6).

In particular, β $rne^-ompT^-lon^-$, featuring the same combination of mutations as BL21 (DE3), showed an improvement in sfGFP-wt expression of 3.7-fold over the parental strain (Figure 3C). The incorporation efficiency of ncAAs into proteins as measured by mass spectrometry also maintained >90% incorporation as seen in the parental strain (Figure S8). When expressing pET28a-sfGFP2UAG with pEVOL-pAzF, β rne^- showed a 1.9-fold improvement over β and 2.3-fold improvement over BL21(DE3). It appears that no matter the RNA polymerase used for expression, rne^- is the most beneficial mutation for expression of sfGFP in $C321.\Delta A$ strains. Lastly, when expressing sfGFP-2UAG with pEVOL-MMpyl, we observed a 17-fold improvement compared to β. In this case, we suspect the highest fold improvement was observed due to the poor solubility of PylRS.

4 | CONCLUSIONS

The genomically recoded strain $C321.\Delta A$ has a fully orthogonal amber codon for site-specific ncAA incorporation into proteins. However, it has not previously been optimized for protein production in vivo. To address this gap, we applied MAGE[53] to generate a series of $C321.\Delta A$ derivatives with combinatorial inactivation of several nucleases and proteases. Protein yield from each strain was quantified as a function of sfGFP fluorescence/O.D.$_{600}$ to assess the impacts of these mutations on protein production. This analysis revealed that the functional inactivation of three targets ($ompT^-rne^-endA^-$) improved sfGFPwt production by ≈2.6-fold, while inactivation of rne and $endA$ improved the production of sfGFP featuring two pAzF residues (sfGFP2pAzF) by ≈2.3-fold. Pushing the limits of the system, inactivation of the Lon protease dramatically improved expression of ELP featuring 10 pAzF residues. Finally, use of the PylRS improved ≈5.6-fold in a top mutant as compared to the parental strain, suggesting applicability of our approach to cases in which mRNA and/or protein stability are known issues.[49,50] Notably, across all trials and experiments the functional inactivation of the RNAse rne was the most impactful.

To introduce precise control of target protein expression via transcriptional tuning, we introduced a synthetic cassette encoding an IPTG-inducible T7RNAP into our strains. When this cassette was inserted into $C321.\Delta A$ prior to the combinatorial inactivation of $ompT$, rne, and lon, improvements of up to 3.7- and 1.9-fold were observed for sfGFPwt and sfGFP2pAzF, respectively, as compared to the parental strain. Incorporation of Pyl also improved significantly in these strains. Importantly, the top performing T7 strains developed in this study all significantly outperformed BL21(DE3) in terms of both yield and ability to incorporate ncAAs at amber codons. In addition, the creation of conditional mutations in $C321.\Delta A$, rather than static inactivation, could expand the utility of $C321.\Delta A$ for biomanufacturing applications, particularly for more complex protein products. However, conditional mutants were not explored in this study.

Looking forward, as our ability to increase efficiencies of OTSs improves, so will the need for optimized strains to produce proteins containing ncAAs. For example, new efforts to engineer tethered ribosomes in cells offer exciting new dimensions for expanding the chemistry of life.[69–73] For instance, Orelle et al. first demonstrated the evolvability of tethered ribosomes by selecting otherwise dominantly lethal rRNA mutations in the peptidyl transferase center that facilitate the translation of problematic protein sequences.[72] This, supported by increases in biomanufacturing, should make possible new avenues in engineering molecular translation systems.[74]

5 | EXPERIMENTAL SECTION

5.1 | Reagents, buffers, and plasmids

Chemicals and media were purchased from Sigma Aldrich unless otherwise designated. Phusion High-Fidelity DNA Polymerase, Taq DNA polymerase with Standard Taq Buffer, T4 DNA ligase, dNTP, Quick-load DNA Ladders, BL21(DE3) and restriction endonuclease were purchased from New England Biolabs. Multipex PCR Kits were purchased from Qiagen. All DNA isolation procedures used Omega DNA isolation kits. All DNA oligonucleotides were purchased from Integrated DNA Technologies. The ncAA pAzF was purchased from P212121 and Pro-Carb was purchased from BioFine. Synthetic E. coli $C321.\Delta A$ (GenBank: CP06698.1) was received from Farren Isaacs. All oligonucleotides used for cloning are shown in Table S2. All vectors were cloned using Gibson Assembly.[75] pLpp5 plasmids were derived from pDTT1 vector.[48] pET vectors were derived from pET28a vectors.

5.2 | Construction of C321.ΔA mutants

The strains in this study were generated from $C321.\Delta A$[76] using mutagenic oligonucleotides via MAGE[60] (Table S2). Cultures were grown in LB-Lennox media (10 g/L Tryptone, 5 g/L Yeast Extract, and 5 g/L NaCl) at 32°C and 250 rpm throughout the MAGE cycle steps.[60] Single, double, several triple and quadruple mutations were made to $endA$, rne, rnb, lon, and $ompT$. MASC PCR[60] was performed to screen for gene mutations by using wild-type forward (-wt-f) or mutant forward (-mut-f) primers and reverse primers (-r; Table S2). Mutant alleles were screened by running PCR products on a 2% agarose gel and confirmed by DNA sequencing by using sequencing primers (Table S2).

5.3 | Growth curves

Overnight cultures of strains were grown in 2X YT (16 g/L Tryptone, 10 g/L Yeast Extract, and 5 g/L NaCl) media at 32°C at 250 rpm and were diluted 1:50 in 100 μl of 2X YT media. Diluted cultures (100 μl) were added to 96-well polystyrene plates (Costar 3370; Corning). The OD$_{600}$ was measured at 10 min intervals for 20 h at 32°C in orbital shaking mode on a SynergyH1 plate reader (Biotek).

For experiments in minimal media, strains were streaked out on plates containing 100 μg/ml of Carbenicillin. Three colonies were picked and grown in 5 ml minimal salts media overnight with 50 μg/ml Carbenicillin. Minimal media was prepared by mixing 200 ml of 5x M9 salts (Sigma), 10 ml of 100 g/L NH_4Cl (pH 7.4), 2 ml of 1 M $MgSO_4$, 12.5 ml of 20% w/v D-glucose, 0.2 ml 0.5 M $CaCl_2$, 1 mg biotin, 0.5 ml of 2 mg/ml thiamine hydrochloride, 1 ml of 15 ml $FeCl_2$ (in 1 M HCl) 1 ml of 15 mg/ml $ZnCl_2$, and 2 ml of 10% w/v yeast extract per liter of media (pH = 7.4). Cells were grown at 32°C in the plate with shaking, and OD_{600} was measured every 10 min for 20 h.[77]

5.4 | Assaying expression of GFP

Strains were freshly transformed with the plasmids of interest. A single colony was inoculated into 5 ml of 2X YT $Kan_{35}Cm_{25}$ media and grown overnight at 32°C, 250 rpm. Overnight cultures were diluted 1:50 into 5 ml of fresh 2X YT media $Kan_{35}Cm_{25}$ in triplicate and grown at 32°C at 250 rpm. OD_{600} was monitored on a Libra S4 spectrophotometer (Biochrom, Cambridge, UK) until OD_{600} 0.6–0.8 at which point cultures were induced. Inducers consisted of either 5 mM ncAA, 1 mM IPTG, and 0.02% arabinose or 0 mM ncAA, 1 mM IPTG, and 0.02% arabinose. Cultures were allowed to express for 20–24 h after induction prior to harvest. To assay fluorescence, overnight cultures were diluted 10-fold in 2X YT media $Kan_{35}Cm_{25}$. The OD_{600} of the 10-fold dilution was measured on a NanoDrop 2000c (Thermo Scientific) and multiplied by 10. A total amount of 100 μl of the 10-fold dilution was added to 96-well polystyrene plates (Costar 3603) in triplicate. Fluorescence of the plates were measured on a Synergy H1 plate reader with a gain of 60. Normalized fluorescence was obtained by dividing fluorescence reading (normalized to 2X YT media $Kan_{35}Cm_{25}$ wells) by OD_{600} read on the NanoDrop 2000c.

5.5 | Construction of T7RNAP cassette

The T7RNAP cassette was assembled from three pieces: a terminator (TM) piece, a T7RNAP piece, a CmR piece (Table S3). To transcriptionally isolate from the cassette, a 5′ terminator was designed upstream of the T7RNAP piece. The strong synthetic terminator (L3S2P21)[78] was selected to avoid potential homology with native terminators during genomic insertion. The terminator was ordered from IDT as a sense and antisense oligonucleotide (Table S2). The T7RNAP part was amplified from *BL21(DE3)* genomic DNA. The T7RNAP PCR was performed using Phusion with EDC408 and EDC323 primers, 5 ng genomic DNA per microliter of PCR reaction, and 3% DMSO at 98°C for 15 min, with 30 cycles of 98°C for 30 s, 55°C for 30 s, and 72°C for 3 min, and a final extension of 72°C for 25 min. The CmR piece PCR was performed using Phusion with EDC413 and EDC414 primers and the pAM552C plasmid[72] at 98°C for 15 min, with 30 cycles of 98°C for 60 s, 55°C for 30 s, and 72°C for 45 s, and a final extension of 72°C for 25 min. The T7RNAP and CmR PCR reactions each received 1 μl of

DpnI per 20 μl of PCR reaction and were incubated at 37°C for 2 h. The PCR reactions were column purified and run on a 0.7% agarose gel at 90V for 45 min. The correct sized band was cut out of the gel and column purified. All three parts were then pooled together at equal molar concentrations (75 ng of DNA total) in an overlap PCR reaction using Phusion, 3% DMSO at 98°C for 10 min, with 15 cycles of 98°C for 30 s, 55°C for 30 s, and 72°C for 4 min, and a final extension of 72°C for 10 min. The overlap PCR was then diluted 20-fold into a second PCR reaction with EDC410 and EDC414 primers at 98°C for 3 min, with 24 cycles of 98°C for 30 s, 55°C for 30 s, and 72°C for 4 min, and a final extension of 72°C for 10 min. PCR reactions were then column purified and run on a 0.7% agarose gel at 90V for 45 min. The correct sized bands were cut out and column purified. Next, 45 bp of genomic insertion site homology was added to the 5′ and 3′ end of the assembled T7RNAP cassette using Phusion and 3% DMSO with JGP139 and JGP140 primers at 98^{0}C for 3 min, with 25 cycles of 98°C for 60 s, 65°C for 30 s, and 72°C for 7 min, and a final extension of 72°C for 10 min. PCR reactions were column purified, run on a 0.7% agarose gel at 90V for 45 min. The correct sized bands were cut out and column purified. The sequence of the fully assembled cassette was confirmed via sequencing.

5.6 | Datsenko-Wanner of T7RNAP cassette

The T7RNAP cassette was inserted using the λ-red homologous recombination method for PCR products.[60,67]

5.7 | Screening for full T7RNAP cassette insertion

Cells that genomically inserted the CmR portion of the cassette grew on the Cm_{34} plates. To screen for full insertion of the cassette, colony PCR was performed. Colonies on the Cm_{34} plate were picked and inoculated into 100 μl LB-L Cm_{25} media in 96-well plates incubated at 32°C, 250 rpm for at least 3 h. The cultures were used as the template in colony PCR reactions. To screen for 5′ portion of T7RNAP a PCR reaction was performed with MASC PCR reactions using JGP173 and JGP292 primers at 95°C for 15 min, with 30 cycles of 95°C for 30 s, 52°C for 30 s, and 72°C for 1 min, and a final extension of 72°C for 10 min. PCR reactions were run on a 2% gel, 110V 45 min. Colony PCR was repeated at a larger scale for the colonies that resulted in a band, reactions were column purified and submitted for sequencing using JGP173, EDC280, and JGP292 primers. Positive sequence hits were screened for the full T7RNAP region being inserted using Multiplex Master Mix with EDC282 and JGP153 primers at 95°C for 15 min, with 30 cycles of 95°C for 30 s, 53°C for 30 s, and 72°C for 1.5 min, and a final extension of 72°C for 10 min. The PCR reaction were run on a 2% agarose gel. Colony PCR was repeated at a larger scale for the colonies that resulted in a band. The reactions were column purified and submitted for sequencing using EDC282, EDC283, EDC284, EDC285, and JGP153 primers.

5.8 | Removing antibiotic resistance marker

Clones with full T7RNAP cassette present then underwent MAGE to remove the CmR gene using a mutagenic oligonucleotide, JGP389, with homology on the 5′ and 3′ end of the CmR gene. After eight cycles of MAGE, overnight cultures were plated on LB plates at 10^{-6} dilutions in LB-L Cb_{50} media. Colonies were replica-plated onto LB-Cb_{100} and LB $Cb_{100}Cm_{34}$ plates and incubated at 32°C overnight. Colonies that grew on LB-Cb_{100} plates and not LB-$Cb_{100}Cm_{34}$ plates underwent PCR using Multiplex Master Mix with EDC413 and JGP211 primers at 95°C for 15 min, with 30 cycles of 95°C for 30 s, 54°C for 30 s, and 72°C for 1.5 min, and a final extension of 72°C for 10 min. For positive hits colonies the PCR reactions were repeated at a larger scale, column purified, and submitted to sequencing with EDC413 and JGP211 primers to confirm the CmR gene was completely removed.

5.9 | Full-length sfGFP purification and quantification

Strains were freshly transformed with the plasmids of interest. A single colony was inoculated into 5 ml of 2X YT media with $Kan_{35}Cm_{25}$ and grown overnight at 32°C at 250 rpm. Overnight cultures were diluted 1:50 into 40 ml of fresh 2X YT media $Kan_{35}Cm_{25}$ and grown at 32°C, 250 rpm. OD_{600} was monitored on a NanoDrop 2000c until OD_{600} 0.6–0.8 at which point cultures were induced with 5 mM ncAA, 1 mM IPTG, and 0.02% arabinose. Cultures were harvested 20 h after induction by pelleting 30 ml of culture at 5000 g for 10 min at 4°C. The pellet was resuspended in 0.8 ml of 1X phosphate-buffered saline (PBS) buffer for every 1 g of wet cell pellet. Cells were lysed at a frequency of 20 kHz and an amplitude of 50% using a Q125 Sonicator (Qsonica) with a 3.75 mm diameter probe[79] for five cycles of 45 s sonication and 59 s sitting on ice. The input energy (Joules) per cycle averaged to 274. Lysed samples were then centrifuged at 21,000 rpm for 10 min at 4°C. Supernatant was collected as the soluble fraction. Full-length sfGFP was purified from the soluble fraction by using a C-terminal strep-tag and 0.2 ml gratify-flow Strep-Tactin Sepharose mini-columns (IBA GmbH). Purified sfGFP was measured using a Quick Start Bradford Kit (BioRad) in biological triplicate and technical triplicate.

5.10 | Mass spectrometry

Proteins for mass spectrometry analysis were purified using Strep-Tactin XT Superflow Resin (IBA) following the manufacturer's protocols. Purified 2TAG-sfGFP was dialyzed into PBS and buffer exchanged at the 2 h, 16 h, and 20 h time points. Proteins were quantified using the Nanodrop 2000c using molecular weights and extinction coefficients calculated by ExPasy ProtParam. A 2 μM solution of purified sfGFP was made using water as the diluent. A total amout of 8 μl of this solution was injected into a Bruker Elute UPLC equipped with an ACQUITY UPLC Peptide BEH C4 Column, 300 Å, 1.7 μm,

2.1 mm × 50 mm (186004495 Waters Corp.) with a 10 mm guard column of identical packing (186004495 Waters) coupled to an Impact-II UHR TOF Mass Spectrometer (Bruker Daltonics). LC-MS methods were then conducted as published previously.[80]

CONFLICT OF INTEREST

M.C.J. has a financial interest in Pearl Bio. M.C.J.'s interests are reviewed and managed by Northwestern University in accordance with their conflict-of-interest policies. All other authors declare no conflicts of interest.

DATA AVAILABILITY STATEMENT

Data available upon request from authors.

ORCID

Ashty S. Karim https://orcid.org/0000-0002-5789-7715
Michael C. Jewett https://orcid.org/0000-0003-2948-6211

REFERENCES

1. Lodish, H., Berk, A., Zipursky, S. L., Matsudaira, P., Baltimore, D., & Darnell, J. (2000). *Molecular Cell Biology* (4th ed.). W. H. Freeman.
2. Macino, G., Coruzzi, G., Nobrega, F. G., Li, M., & Tzagoloff, A. (1979). Use of the UGA terminator as a tryptophan codon in yeast mitochondria. *Proceedings of the National Academy of Sciences of the United States of America*, 76, 3784–3785, https://doi.org/10.1073/pnas.76.8.3784.
3. Ambrogelly, A., Palioura, S., & Söll, D. (2007). Natural expansion of the genetic code. *Nature Chemical Biology*, 3, 29–35, https://doi.org/10.1038/nchembio847.
4. Arranz-Gibert, P., Vanderschuren, K., & Isaacs, F. (2018). Next-generation genetic code expansion. *Current Opinion in Chemical Biology*, 46, 203–211, https://doi.org/10.1016/j.cbpa.2018.07.020.
5. Bogart, J. W., Cabezas, M. D., Vögeli, B., Wong, D. A., Karim, A. S., & Jewett, M. C. (2021). Cell-free exploration of the natural product chemical space. *Chembiochem*, 22, 84–91, https://doi.org/10.1002/cbic.202000452.
6. Chin, J. W., Expanding and reprogramming the genetic code. *Nature* (2017). 550, Art. no. 7674, https://doi.org/10.1038/nature24031.
7. Hammerling, M. J., Krüger, A., & Jewett, M. C. (2020). Strategies for in vitro engineering of the translation machinery. *Nucleic Acids Research*, 48, 1068–1083, https://doi.org/10.1093/nar/gkz1011.
8. Tharp, J. M., Krahn, N., Varshney, U., & Söll, D. (2020). Hijacking translation initiation for synthetic biology. *Chembiochem*, 21, 1387–1396, https://doi.org/10.1002/cbic.202000017.
9. Darren L, B., Dennis A, D., & Henry A, L. (2003). Unnatural amino acid mutagenesis in mapping ion channel function. *Current Opinion in Neu-*

robiology, *13*(3), 264–270, https://doi.org/10.1016/s0959-4388(03)00068-0.

10. Cornish, V., Mendel, D., & Schultz, P. (1995). Probing protein structure and function with an expanded genetic code. *Angewandte Chemie International Edition in English*, *34*, 621–633.

11. Yu, Y., Zhou, Q., Wang, L., Liu, X., Zhang, W., Hu, M., Dong, J., Li, J., Lv, X., Ouyang, H., Li, H., Gao, F., Gong, W., Lu, Y., & Wang, J. (2015). Significant improvement of oxidase activity through the genetic incorporation of a redox-active unnatural amino acid. *Chemical Science*, *6*, 3881–3885, https://doi.org/10.1039/C5SC01126D.

12. Liu, H., Wang, L., Brock, A., Wong, C. - H., & Schultz, P. G. (2003). A method for the generation of glycoprotein mimetics. *Journal of the American Chemical Society*, *125*(7), 1702–1703, https://doi.org/10.1021/ja029433n.

13. Oza, J. P., Aerni, H. R., Pirman, N. L., Barber, K. W., ter Haar, C. M., Rogulina, S., Amrofell, M. B., Isaacs, F. J., Rinehart, J., & Jewett, M. C. (2015). Robust production of recombinant phosphoproteins using cell-free protein synthesis. *Nature Communications*, *6*, Art. no. 1, 8168. https://doi.org/10.1038/ncomms9168.

14. Pirman, N. L., Barber, K. W., Aerni, H. R., Ma, N. J., Haimovich, A. D., Rogulina, S., Isaacs, F. J., & Rinehart, J. (2015). A flexible codon in genomically recoded Escherichia coli permits programmable protein phosphorylation. *Nature Communications*, *6*, Art. no. 1, https://doi.org/10.1038/ncomms9130.

15. Hammerling, M. J., Ellefson, J. W., Boutz, D. R., Marcotte, E. M., Ellington, A. D., & Barrick, J. E. (2014). Bacteriophages use an expanded genetic code on evolutionary paths to higher fitness. *Nature Chemical Biology*, *10*, 178–180, https://doi.org/10.1038/nchembio.1450.

16. O'Donoghue, P., Ling, J., Wang, Y.-S., & Söll, D. (2013). Upgrading protein synthesis for synthetic biology. *Nature Chemical Biology*, *9*, 594–598, https://doi.org/10.1038/nchembio.1339.

17. Soye, B. J. D., Patel, J. R., Isaacs, F. J., & Jewett, M. C. (2015). Repurposing the translation apparatus for synthetic biology. *Current Opinion in Chemical Biology*, *28*, 83–90, https://doi.org/10.1016/j.cbpa.2015.06.008.

18. Katoh, T., Sengoku, T., Hirata, K., Ogata, K., & Suga, H. (2020). Ribosomal synthesis and de novo discovery of bioactive foldamer peptides containing cyclic β^2-amino acids. *Nature Chemistry*, *12*, Art. no. 11, 1081. https://doi.org/10.1038/s41557-020-0525-1.

19. Katoh, T., & Suga, H. (2020). Ribosomal elongation of cyclic γ^3-amino acids using a reprogrammed genetic code. *Journal of the American Chemical Society*, *142*, 4965–4969, https://doi.org/10.1021/jacs.9b12280.

20. Katoh, T., Tajima, K., & Suga, H. (2017). Consecutive elongation of D-amino acids in translation. *Cell Chemical Biology*, *24*, 46–54, https://doi.org/10.1016/j.chembiol.2016.11.012.

21. Fujino, T., Goto, Y., Suga, H., & Murakami, H. (2016). Ribosomal synthesis of peptides with multiple β^2-amino acids. *Journal of the American Chemical Society*, *138*(6), 1962–1969, https://doi.org/10.1021/jacs.5b12482.

22. Lee, J., Schwarz, K. J., Yu, H., Krüger, A., Anslyn, E. V., Ellington, A. D., Moore, J. S., & Jewett, M. C. (2021). Ribosome-mediated incorporation of fluorescent amino acids into peptides in vitro. *Chemical Communications*, *57*, 2661–2664, https://doi.org/10.1039/D0CC07740B.

23. Lee, J., Schwarz, K. J., Kim, D. S., Moore, J. S., & Jewett, M. C. (2020). Ribosome-mediated polymerization of long chain carbon and cyclic amino acids into peptides in vitro. *Nature Communications*, *11*, Art. no. 1, 1. https://doi.org/10.1038/s41467-020-18001-x.

24. Lee, J., Schwieter, K. E., Watkins, A. M., Kim, D. S., Yu, H., Schwarz, K. J., Lim, J., Coronado, J., Byrom, M., Anslyn, E. V., Ellington, A. D., Moore, J. S., & Jewett, M. C. (2019). Expanding the limits of the second genetic code with ribozymes. *Nature Communications*, *10*, 5097, https://doi.org/10.1038/s41467-019-12916-w.

25. Lee, J., Torres, R., Kim, D. S., Byrom, M., Ellington, A. D., & Jewett, M. C. (2020). Ribosomal incorporation of cyclic β^2-amino acids into peptides

using in vitro translation. *Chemical Communications*, *56*, 5597–5600, https://doi.org/10.1039/D0CC02121K.

26. Rogers, J. M., Kwon, S., Dawson, S. J., Mandal, P. K., Suga, H., & Huc, I. (2018). Ribosomal synthesis and folding of peptide-helical aromatic foldamer hybrids. *Nature Chemistry*, *10*, 405–412, https://doi.org/10.1038/s41557-018-0007-x.

27. Takatsuji, R., Shinbara, K., Katoh, T., Goto, Y., Passioura, T., Yajima, R., Komatsu, Y., & Suga, H. (2019). Ribosomal synthesis of backbone-cyclic peptides compatible with in vitro display. *Journal of the American Chemical Society*, *141*, 2279–2287, https://doi.org/10.1021/jacs.8b05327.

28. Kakkar, N., Perez, J. G., Liu, W. R., Jewett, M. C., & van der Donk, W. A. (2018). Incorporation of nonproteinogenic amino acids in Class I and II lantibiotics. *Acs Chemical Biology*, *13*, 951–957, https://doi.org/10.1021/acschembio.7b01024.

29. Ryu, Y., & Schultz, P. G. (2006). Efficient incorporation of unnatural amino acids into proteins in *Escherichia coli*. *Nature Methods*, *3*, 263–265, https://doi.org/10.1038/nmeth864.

30. Santoro, S. W., Wang, L., Herberich, B., King, D. S., & Schultz, P. G. (2002). An efficient system for the evolution of aminoacyl-tRNA synthetase specificity. *Nature Biotechnology*, *20*, 1044–1048, https://doi.org/10.1038/nbt742.

31. Young, T. S., Ahmad, I., Yin, J. A., & Schultz, P. G. (2010). An enhanced system for unnatural amino acid mutagenesis in *E. coli*. *Journal of Molecular Biology*, *395*, 361–374, https://doi.org/10.1016/j.jmb.2009.10.030.

32. Griffiths, A., Doebley, J., Peichel, C., & Wassarman, D. (2020). *Introduction to genetic analysis* (12th ed.). Macmillan.

33. Isaacs, F. J., Carr, P. A., Wang, H. H., Lajoie, M. J., Sterling, B., Kraal, L., Tolonen, A. C., Gianoulis, T. A., Goodman, D. B., Reppas, N. B., Emig, C. J., Bang, D., Hwang, S. J., Jewett, M. C., Jacobson, J. M., & Church, G. M. (2011). Precise manipulation of chromosomes in vivo enables genome-wide codon replacement. *Science*, *333*, 348–353, https://doi.org/10.1126/science.1205822.

34. Robertson, W. E., Funke, L. F. H., de la Torre, D., Fredens, J., Elliott, T. S., Spinck, M., Christova, Y., Cervettini, D., Böge, F. L., Liu, K. C., Buse, S., Maslen, S., Salmond, G. P. C., & Chin, J. W. (2021). Sense codon reassignment enables viral resistance and encoded polymer synthesis. *Science*, *372*, 1057–1062, https://doi.org/10.1126/science.abg3029.

35. Fredens, J., Wang, K., de la Torre, D., Funke, L. F. H., Robertson, W. E., Christova, Y., Chia, T., Schmied, W. H., Dunkelmann, D. L., Beránek, V., Uttamapinant, C., Llamazares, A. G., Elliott, T. S., & Chin, J. W. (2019). Total synthesis of *Escherichia coli* with a recoded genome. *Nature*, *569*, 514–518, https://doi.org/10.1038/s41586-019-1192-5.

36. Hong, S. H., Kwon, Y. - C., Martin, R. W., Des Soye, B. J., de Paz, A. M., Swonger, K. N., Ntai, I., Kelleher, N. L., & Jewett, M. C. (2015). improving cell-free protein synthesis through genome engineering of *Escherichia coli* lacking release Factor 1. *Chembiochem*, *16*, 844–853, https://doi.org/10.1002/cbic.201402708.

37. Amiram, M., Haimovich, A. D., Fan, C., Wang, Y. - S., Aerni, H. - R., Ntai, I., Moonan, D. W., Ma, N. J., Rovner, A. J., Hong, S. H., Kelleher, N. L., Goodman, A. L., Jewett, M. C., Söll, D., Rinehart, J., & Isaacs, F. J. (2015). Evolution of translation machinery in recoded bacteria enables multi-site incorporation of nonstandard amino acids. *Nature Biotechnology*, *33*, 1272–1279, https://doi.org/10.1038/nbt.3372.

38. Mandell, D. J., Lajoie, M. J., Mee, M. T., Takeuchi, R., Kuznetsov, G., Norville, J. E., Gregg, C. J., Stoddard, B. L., & Church, G. M. (2015). Biocontainment of genetically modified organisms by synthetic protein design. *Nature*, *518*, 55–60, https://doi.org/10.1038/nature14121.

39. Gopal, G. J., & Kumar, A. (2013). Strategies for the production of recombinant protein in *Escherichia coli*. *The Protein Journal*, *32*, 419–425, https://doi.org/10.1007/s10930-013-9502-5.

40. Makino, T., Skretas, G., & Georgiou, G. (2011). Strain engineering for improved expression of recombinant proteins in bacteria. *Microbial Cell Factories*, *10*, 32, https://doi.org/10.1186/1475-2859-10-32.

41. Martin, R. W., Des Soye, B. J., Kwon, Y.-C., Kay, J., Davis, R. G., Thomas, P. M., Majewska, N. I., Chen, C. X., Marcum, R. D., Weiss, M. G., Stoddart, A. E., Amiram, M., Ranji Charna, A. K., Patel, J. R., Isaacs, F. J., Kelleher, N. L., Hong, S. H., & Jewett, M. C. (2018). Cell-free protein synthesis from genomically recoded bacteria enables multisite incorporation of noncanonical amino acids. *Nature Communications*, *9*, Art. no. 1, https://doi.org/10.1038/s41467-018-03469-5.

42. Borja, G. M., Meza Mora, E., Barrón, B., Gosset, G., Ramírez, O. T., & Lara, A. R. (2012). Engineering *Escherichia coli* to increase plasmid DNA production in high cell-density cultivations in batch mode. *Microbial Cell Factories*, *11*, 132, https://doi.org/10.1186/1475-2859-11-132.

43. Lopez, P. J., Marchand, I., Joyce, S. A., & Dreyfus, M. (1999). The C-terminal half of RNase E, which organizes the *Escherichia coli* degradosome, participates in mRNA degradation but not rRNA processing in vivo. *Molecular Microbiology*, *33*, 188–199, https://doi.org/10.1046/j.1365-2958.1999.01465.x.

44. Kaplan, R., & Apirion, D. (1974). the involvement of ribonuclease I, ribonuclease II, and polynucleotide phosphorylase in the degradation of stable ribonucleic acid during carbon starvation in *Escherichia coli*. *Journal of Biological Chemistry*, *249*, 149–151.

45. Deutscher, M. P. (1985). E. coli RNases: Making sense of alphabet soup *Cell*, *40*, 731–732, https://doi.org/10.1016/0092-8674(85)90330-7.

46. Studier, F. W., & Moffatt, B. A. (1986). Use of bacteriophage T7 RNA polymerase to direct selective high-level expression of cloned genes. *Journal of Molecular Biology*, *189*, 113–130, https://doi.org/10.1016/0022-2836(86)90385-2.

47. Moatsou, D., Li, J., Ranji, A., Pitto-Barry, A., Ntai, I., Jewett, M. C., & O'Reilly, R. K. (2015). Self-assembly of temperature-responsive protein-polymer bioconjugates. *Bioconjugate Chemistry*, *26*(9), 1890–1899, https://doi.org/10.1021/acs.bioconjchem.5b00264.

48. Gan, R., Perez, J. G., Carlson, E. D., Ntai, I., Isaacs, F. J., Kelleher, N. L., & Jewett, M. C. (2016). Translation system engineering in *Escherichia coli* enhances non-canonical amino acid incorporation into proteins. *Biotechnology and Bioengineering*, *114*, 1074–1086, https://doi.org/10.1002/bit.26239.

49. Yanagisawa, T., Ishii, R., Fukunaga, R., Nureki, O., & Yokoyama, S. (2006). Crystallization and preliminary X-ray crystallographic analysis of the catalytic domain of pyrrolysyl-tRNA synthetase from the methanogenic archaeon Methanosarcina mazei. *Acta Crystallographica Section F: Structural Biology and Crystallization Communications*, *62*, 1031–1033, https://doi.org/10.1107/S1744309106036700.

50. Jiang, R., & Krzycki, J. A., PylSn and the homologous N-terminal domain of pyrrolysyl-tRNA synthetase bind the trna that is essential for the genetic encoding of pyrrolysine. *Journal of Biological Chemistry*, *287*, 32738–32746, 2012, https://doi.org/10.1074/jbc.M112.396754.

51. Baneyx, F. (1999). Recombinant protein expression in Escherichia coli. *Current Opinion in Biotechnology*, *10*, 411–421, https://doi.org/10.1016/s0958-1669(99)00003-8.

52. Graumann, K., & Premstaller, A. (2006). Manufacturing of recombinant therapeutic proteins in microbial systems. *Biotechnology Journal*, *1*, 164–186, https://doi.org/10.1002/biot.200500051.

53. Wang, H. H., Isaacs, F. J., Carr, P. A., Sun, Z. Z., Xu, G., Forest, C. R., & Church, G. M. (2009). Programming cells by multiplex genome engineering and accelerated evolution. *Nature*, *460*, 894–898, https://doi.org/10.1038/nature08187.

54. SaiSree, L., Reddy, M., & Gowrishankar, J. (2001). IS 186 insertion at a hot spot in the lon promoter as a basis for lon protease deficiency of *Escherichia coli* B: Identification of a consensus target sequence for IS 186 transposition. *Journal of Bacteriology*, *183*(23), 6943–6946, https://doi.org/10.1128/JB.183.23.6943-6946.2001.

55. Goerke, A., & Swartz, J., WO-2008066583-A3, 2008 [Online]. Available: https://patentscope.wipo.int/search/en/detail.jsf?docId=WO2008066583

56. Spiess, C., Beil, A., & Ehrmann, M. (1999). A temperature-dependent switch from chaperone to protease in a widely conserved heat shock protein. *Cell*, *97*, 339–347, https://doi.org/10.1016/s0092-8674(00)80743-6.

57. Kido, M., Yamanaka, K., Mitani, T., Niki, H., Ogura, T., & Hiraga, S. (1996). RNase E polypeptides lacking a carboxyl-terminal half suppress a mukB mutation in Escherichia coli. *Journal of Bacteriology*, *178*, 3917–3925, https://doi.org/10.1128/jb.178.13.3917-3925.1996.

58. Donovan, W. P., & Kushner, S. R. (1986). Polynucleotide phosphorylase and ribonuclease II are required for cell viability and mRNA turnover in *Escherichia coli* K-12. *Proceedings of the National Academy of Sciences of the United States of America*, *83*, 120–124, https://doi.org/10.1073/pnas.83.1.120.

59. Bermardo, G., & Cordonnier, C. (1965). Mechanism of degradation of DNA by endonuclease I from *Escherichia coli*. *Journal of Molecular Biology*, *11*, 141–143, https://doi.org/10.1016/s0022-2836(65)80180-2.

60. Wang, H. H., & Church, G. M. (2011). Multiplexed genome engineering and genotyping methods: Applications for synthetic biology and metabolic engineering. *Methods in Enzymology*, *498*, 409–426, https://doi.org/10.1016/B978-0-12-385120-8.00018-8.

61. Kushner, S. R. (2002). mRNA decay in *Escherichia coli* comes of age. *Journal of Bacteriology*, *184*, 4658–4665, https://doi.org/10.1128/JB.184.17.4658-4665.2002.

62. Studier, F. W., Daegelen, P., Lenski, R. E., Maslov, S., & Kim, J. F. (2009). Understanding the differences between genome sequences of *Escherichia coli* B strains REL606 and BL21(DE3) and comparison of the *E. coli* B and K-12 genomes. *Journal of Molecular Biology*, *394*, 653–680, https://doi.org/10.1016/j.jmb.2009.09.021.

63. Inouye, S., & Inouye, M. (1985). Up-promoter mutations in the lpp gene of Escherichia coli. *Nucleic Acids Research*, *13*(9), 3101–3110. https://doi.org/10.1093/nar/13.9.3101.

64. Hong, S. H., Ntai, I., Haimovich, A. D., Kelleher, N. L., Isaacs, F. J., & Jewett, M. C. (2014). Cell-free protein synthesis from a release Factor 1 deficient *Escherichia coli* activates efficient and multiple site-specific nonstandard amino acid incorporation. *ACS Synthetic Biology*, *3*, 398–409, https://doi.org/10.1021/sb400140t.

65. Srinivasan, G., James, C. M., & Krzycki, J. A. (2002). Pyrrolysine encoded by UAG in Archaea: Charging of a UAG-decoding specialized tRNA. *Science*, *296*, 1459–1462, https://doi.org/10.1126/science.1069588.

66. Hao, B., Zhao, G., Kang, P. T., Soares, J. A., Ferguson, T. K., Gallucci, J., Krzycki, J. A., & Chan, M. K. (2004). Reactivity and chemical synthesis of L-pyrrolysinethe 22nd genetically encoded amino acid. *Chemistry & Biology*, *11*(9), 1317–1324, https://doi.org/10.1016/j.chembiol.2004.07.011.

67. Datsenko, K. A., & Wanner, B. L. (2000). One-step inactivation of chromosomal genes in *Escherichia coli* K-12 using PCR products. *Proceedings of the National Academy of Sciences of the United States of America*, *97*, 6640–6645, https://doi.org/10.1073/pnas.120163297.

68. Reim, R. L., Narula, S. K., Ryan, M. J. & Leibowitz, P. J. Expression systems utilizing bacteriophage t7 promoters, gene sequences, and t7 rna polymerase. U.S. Patent 5,122,457, issued June 16, 1992. Available: https://patents.google.com/patent/AU7043491A/en

69. Aleksashin, N. A., Leppik, M., Hockenberry, A. J., Klepacki, D., Vázquez-Laslop, N., Jewett, M. C., Remme, J., & Mankin, A. S. (2019). Assembly and functionality of the ribosome with tethered subunits. *Nature Communications*, *10*(1), https://doi.org/10.1038/s41467-019-08892-w.

70. Yesselman, J. D., Eiler, D., Carlson, E. D., Gotrik, M. R., d'Aquino, A. E., Ooms, A. N., Kladwang, W., Carlson, P. D., Shi, X., Costantino, D. A., Herschlag, D., Lucks, J. B., Jewett, M. C., Kieft, J. S., & Das, R. (2019). Computational design of three-dimensional RNA structure and function. *Nature Nanotechnology*, *14*, 866–873, https://doi.org/10.1038/s41565-019-0517-8.

71. Aleksashin, N. A., Szal, T., d'Aquino, A. E., Jewett, M. C., Vázquez-Laslop, N., & Mankin, A. S. (2020). A fully orthogonal system for protein synthesis in bacterial cells. *Nature Communications*, *11*, Art. no. 1, https://doi.org/10.1038/s41467-020-15756-1.

72. Orelle, C., Carlson, E. D., Szal, T., Florin, T., Jewett, M. C., & Mankin, A. S. (2015). Protein synthesis by ribosomes with tethered subunits. *Nature*, *524*, 119–124, https://doi.org/10.1038/nature14862.

73. Carlson, E. D., d'Aquino, A. E., Kim, D. S., Fulk, E. M., Hoang, K., Szal, T., Mankin, A. S., & Jewett, M. C. (2019). Engineered ribosomes with tethered subunits for expanding biological function. *Nature Communications*, *10*, 3920, https://doi.org/10.1038/s41467-019-11427-y.

74. Kofman, C., Lee, J., & Jewett, M. C. (2021). Engineering molecular translation systems. *Cell Systems*, *12*, 593–607, https://doi.org/10.1016/j.cels.2021.04.001.

75. Gibson, D. G., Young, L., Chuang, R. - Y., Venter, J. C., Hutchison, C. A., & Smith, H. O. (2009). Enzymatic assembly of DNA molecules up to several hundred kilobases. *Nature Methods*, *6*, 343–345, https://doi.org/10.1038/nmeth.1318.

76. Lajoie, M. J., Rovner, A. J., Goodman, D. B., Aerni, H. - R., Haimovich, A. D., Kuznetsov, G., Mercer, J. A., Wang, H. H., Carr, P. A., Mosberg, J. A., Rohland, N., Schultz, P. G., Jacobson, J. M., Rinehart, J., Church, G. M., & Isaacs, F. J. (2013). Genomically recoded organisms expand biological functions. *Science*, *342*, 357–360, https://doi.org/10.1126/science.1241459.

77. Swain, P. S., Stevenson, K., Leary, A., Montano-Gutierrez, L. F., Clark, I. B. N., Vogel, J., & Pilizota, T. (2016). Inferring time derivatives including cell growth rates using Gaussian processes. *Nature Communications*, *7*, 13766, https://doi.org/10.1038/ncomms13766.

78. Chen, Y.-J., Liu, P., Nielsen, A. A. K., Brophy, J. A. N., Clancy, K., Peterson, T., & Voigt, C. A. (2013). Characterization of 582 natural and synthetic terminators and quantification of their design constraints. *Nature Methods*, *10*, 659–664, https://doi.org/10.1038/nmeth.2515.

79. Kwon, Y.-C., & Jewett, M. C. (2015). High-throughput preparation methods of crude extract for robust cell-free protein synthesis. *Science Reports*, *5*(1), https://doi.org/10.1038/srep08663.

80. Kightlinger, W., Duncker, K. E., Ramesh, A., Thames, A. H., Natarajan, A., Stark, J. C., Yang, A., Lin, L., Mrksich, M., DeLisa, M. P., & Jewett, M. C. (2019). A cell-free biosynthesis platform for modular construction of protein glycosylation pathways. *Nature Communications*, *10*, 5404, https://doi.org/10.1038/s41467-019-12024-9.

SUPPORTING INFORMATION

Additional supporting information may be found in the online version of the article at the publisher's website.